

Asymmetries in foveal vision

Samantha K. Jenks^{1,3}, Marisa Carrasco^{4,5}, and Martina Poletti*
email: martina_poletti@urmc.rochester.edu ^{1,2,3}

¹Department of Brain and Cognitive Sciences, University of Rochester

²Department of Neuroscience, University of Rochester

³Center for Visual Science, University of Rochester

⁴Department of Psychology, New York University

⁵Center for Neural Science, New York University

Abstract: Visual perception is characterized by known asymmetries in the visual field; human's visual sensitivity is higher along the horizontal than the vertical meridian, and along the lower than the upper vertical meridian. These asymmetries decrease with decreasing eccentricity from the periphery to the center of gaze, suggesting that they may be absent in the 1-deg foveola, the retinal region used to explore scenes at high-resolution. Using high-precision eyetracking and gaze-contingent display, allowing for accurate control over the stimulated foveolar location despite the continuous eye motion at fixation, we investigated fine visual discrimination at different isoeccentric locations across the foveola and parafovea. Although the tested foveolar locations were only 0.3 deg away from the center of gaze, we show that, similar to more eccentric locations, humans are more sensitive to stimuli presented along the horizontal than the vertical meridian. Whereas the magnitude of this asymmetry is reduced in the foveola, the magnitude of the vertical meridian asymmetry is comparable but, interestingly, reversed: objects presented slightly above the center of gaze are more easily discerned than when presented at the same eccentricity below the center of gaze. Therefore, far from being uniform, as often assumed, foveolar vision is characterized by perceptual asymmetries. Further, these asymmetries differ not only in magnitude but also in direction compared to those present just ~ 4 deg away from the center of gaze, resulting in overall different foveal and extrafoveal perceptual fields.

Introduction

It is well established that perception across the visual field is not uniform. As eccentricity increases, visual acuity^{1,2,3}, contrast sensitivity^{4,5}, object recognition⁶, and cortical magnification –the amount of cortical surface

area corresponding to one degree of visual angle^{7,8,9}— decline. Several factors contribute to this decline, including an increase in retinal cone^{10,11,12} and retinal ganglion cell^{13,14} spacing, as well as an increase in the population receptive field (pRF) size in the visual cortex^{15,16}. It is, however, less known that vision is not uniform at isoeccentric locations (polar angle) along a given eccentricity (see¹⁷ for a review). In particular, sensitivity differs at isoeccentric locations at the same eccentricity. This phenomenon is referred to as visual asymmetries (e.g.,^{18,19,20,21,22,23,24,25,26,27}).

There are two well-studied visual asymmetries in the extrafoveal visual field: the *horizontal-vertical meridian asymmetry*, characterized by greater sensitivity along the horizontal than the vertical meridian, and the *vertical meridian asymmetry*, characterized by greater sensitivity along the lower than the upper vertical meridian (e.g.,^{18,19,20,21,22,23,24,25,26,27}). These asymmetries have been assessed in many basic visual tasks, such as contrast sensitivity^{18,19,21,23,26}, texture segmentation²⁸, and acuity^{29,30,31}. Interestingly, the extent of these asymmetries increases with higher stimulus spatial frequency^{18,26,29} and with increasing eccentricity from the center of gaze^{18,24,32}. It has also been shown that asymmetry is the strongest along the meridian, but gradually diminishes with angular distance from the meridian^{23,24,29}. These changes create a continuous field of gradually varying sensitivity, referred to as the performance field (e.g.,^{33,18,19}).

These visual asymmetries have also been reported in more complex tasks such as letter identification task³³ visually guided pointing³⁴, motion discrimination³⁵, numerosity³⁶, perceived size³⁷, and visual short-term memory³⁸. Furthermore, visual asymmetries persist even when spatial attention—both exogenous^{18,19,28,39,40} and endogenous^{41,42}— or temporal attention⁴³ is engaged. Therefore, visual asymmetries are pervasive and shape multiple aspects of visual processing.

These visual asymmetries have been extensively studied in the extrafoveal visual field, yet it is unknown whether these asymmetries extend to the foveola. The foveola receives input from the central 1-degree of the visual field⁴⁴. This region is responsible for high-resolution vision; it is defined by being devoid of capillaries and rods, and it is characterized by the highest cone density and spatial resolution. Therefore, the foveola is of paramount importance in many everyday tasks such as reading, driving, and discriminating stimuli from a distance. Further, although the foveola covers less than 0.01% of the visual field, its input is over-represented by ≈ 800 times in the primary visual cortex⁴⁵. Yet, foveolar vision is often assumed to be characterized by uniformly high sensitivity and is generally treated as a single homogeneous region.

Based on evidence that the magnitude of visual asymmetries decreases at near eccentricities^{18,24,46} and that spotlight sensitivity for isoeccentric locations in the foveolar field is uniform⁴⁷, we may expect no asymmetries in visual discrimination within the central 1-degree of the visual field, where acuity, under normal viewing conditions, is primarily limited by uniform optics^{48,49,50}. However, evidence showing that fine spatial vision already starts to decline across the central fovea^{51,52}, and that retinal cone density along the vertical meridian of the foveola declines with eccentricity more pronouncedly than along the horizontal meridian^{10,14,12} would suggest otherwise.

Assessing visual asymmetries at the foveolar scale requires precise localization of the line of sight, with arcminute level accuracy, to present small stimuli at predefined eccentricities from the preferred locus of fixation, a capability that exceeds what commercial video-eyetrackers can achieve⁵³. To overcome these issues and investigate fine visual discrimination at isoeccentric locations in the foveola, we relied on a custom-made high-precision Dual Purkinje Image eyetracker⁵⁴ coupled with a gaze contingent display system⁵⁵. Together, these systems enable the recording of eye movements with high precision and provide a more accurate localization of the line of sight^{54,56}.

Results

Visual asymmetries are defined as differences in visual perception (e.g., visual sensitivity and acuity) at different polar angles along a given eccentricity. Whereas asymmetries in the parafovea and perifovea have been extensively studied, it is not yet known whether asymmetries are present in the 1 deg central fovea. To investigate this issue, fine spatial discrimination was tested at eight isoeccentric locations in the foveola (4 cardinal and 4 intercardinal), ≈ 20 arcminutes away from the preferred locus of fixation (Foveolar condition, Fig. 1A–B). As a comparison, performance was also assessed at the corresponding locations in the parafovea at 4.5 deg eccentricity (Parafoveal condition). Observers were asked to maintain fixation on a central marker while discriminating the orientation of a tiny bar (tilted ± 45 deg) that was briefly presented at one of the tested locations (Fig. 1A). To maintain comparable task difficulty between the foveal and parafoveal conditions, stimulus contrast was adjusted to yield an overall performance $\approx 70\%$ of correct responses across the 8 tested locations in each condition ($t(7) = -0.61$, $p = 0.56$, paired two-tailed t-test; $BF = 2.54$ for the null hypothesis; Fig. 1C).

Testing fine spatial vision within the foveola is challenging because it is difficult to present and maintain stimuli at the desired location, only arcminutes away from the preferred locus of fixation. During fixation, eye movements continually shift the retinal projections of objects across the foveola, even during brief fixation periods^{58,59}. Here, we used a high-precision eyetracker⁵⁴ and a gaze contingent display⁵⁵ to more accurately localize the line of sight and to either present stimuli at a fixed eccentricity using retinal stabilization, or to post-hoc select only trials in which gaze position was maintained within a circular region of 10 arcminutes in radius around the center of the display ($10\% \pm 7\%$ of trials in the foveola were removed post-hoc for gaze off center). Figure 1D shows that in the latter case, the average target distance from the preferred locus of fixation remained approximately at the desired eccentricity of $20' \pm 3'$, and it was comparable across all tested locations ($N=10$, $F(7,9) = 1.93$, $p = 0.08$, one-way ANOVA; $BF = 1.56$ for the null hypothesis). Retinal stabilization was used only for two subjects who showed larger fixational instability (see Methods for details).

Despite the stimuli being presented at isoeccentric locations, performance was not uniform across the eight tested locations both in the parafovea ($F(7,7) = 12.21$, $p < 0.0001$, one-way ANOVA; $BF > 100$) and in the foveola ($F(7,11) = 4.95$, $p = 0.0001$, one-way ANOVA; $BF > 100$). Consistent with previous literature

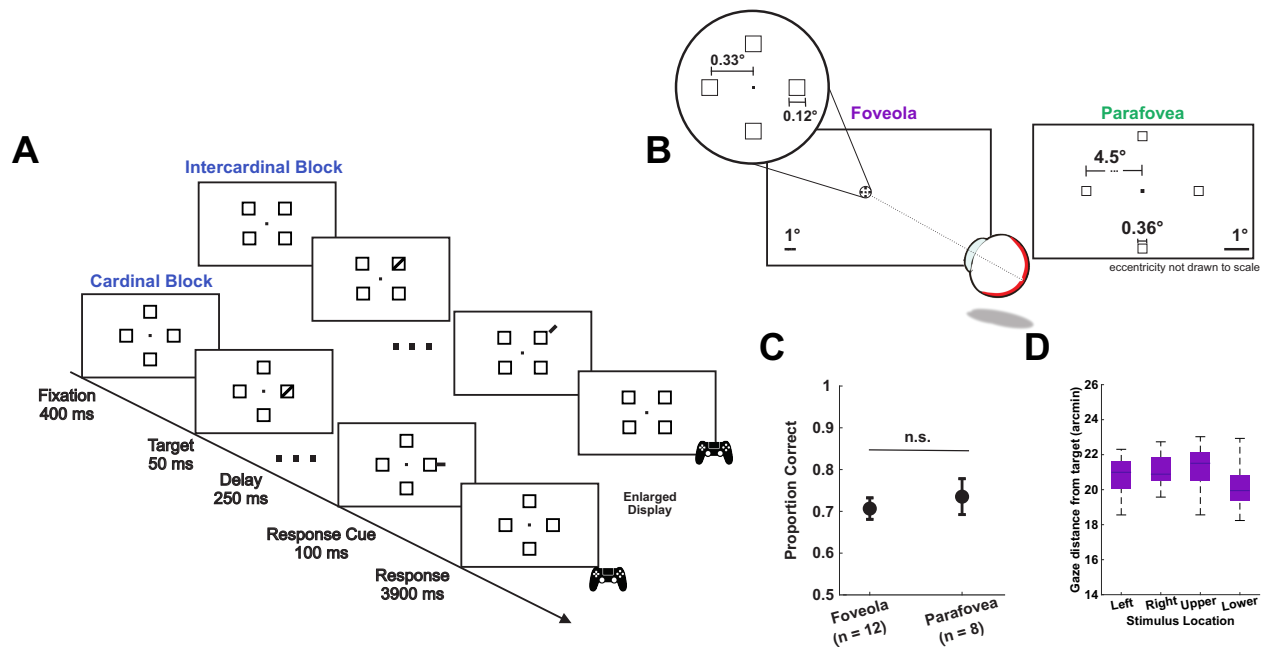


Figure 1: **Experimental protocol.** **A-** Subjects fixated monocularly (left eye patched) on a central fixation marker while stimuli were presented. The target, a small bar tilted ± 45 deg, appeared briefly (50ms) at one of 4 possible locations and subjects were asked to report its orientation once the response cue was presented. A total of eight locations were tested. Cardinal and intercardinal locations were tested in separate blocks. **B-** Stimuli spatial arrangement and dimensions in the foveola (left; $n = 12$) and parafovea (right; $n = 8$) conditions. In the latter condition, stimuli were magnified according to the cortical magnification factor⁵⁷. **C-** In a preliminary session, the stimulus contrast was determined for the foveola and the parafovea conditions separately, so that overall performance across cardinal and intercardinal locations yielded $\approx 70\%$ correct responses. Error bars are 95% confidence intervals. **D-** The target was 20 arcmin from the center of the display. The box and whisker plot shows that the average gaze distance from the target was approximately 20 arcminutes for different target locations in the foveola condition.

(e.g.,^{33,18,19,24,37,26,29,60,36}), in the parafoveal condition, we found the typical horizontal-vertical meridian asymmetry in performance; subjects were on average $27\% \pm 12\%$ better at discriminating stimuli along the horizontal than the vertical meridian (Figure 2A–B; horizontal = $91\% \pm 4\%$; vertical = $64\% \pm 3\%$; two-tailed paired t-test: $t(7) = 6.37$, $p = 0.0004$; BF = 91.22; Cohen's $d = 3.44$). Interestingly, when stimuli were presented foveally, a similar pattern was found (Figure 2A; horizontal: $74\% \pm 4\%$; vertical: $68\% \pm 3\%$; two-tailed paired t-test: $t(11) = 2.71$, $p = 0.02$; BF = 3.36; Cohen's $d = 0.94$). This asymmetry was present for all individual subjects in the parafovea and for most subjects in the foveola (Figure 2B). However, the magnitude of this asymmetry was 4.4 times larger in the parafovea than in the central fovea (Figure 2C). These results are consistent with the findings that asymmetries increase with eccentricity^{18,24,46}.

In the parafoveal condition, both locations along the vertical meridian showed a significant drop in performance compared to those along the horizontal meridian ($F(2,7) = 37.33$, $p < 0.0001$; BF = 5.51; horizontal: $91\% \pm 4\%$;

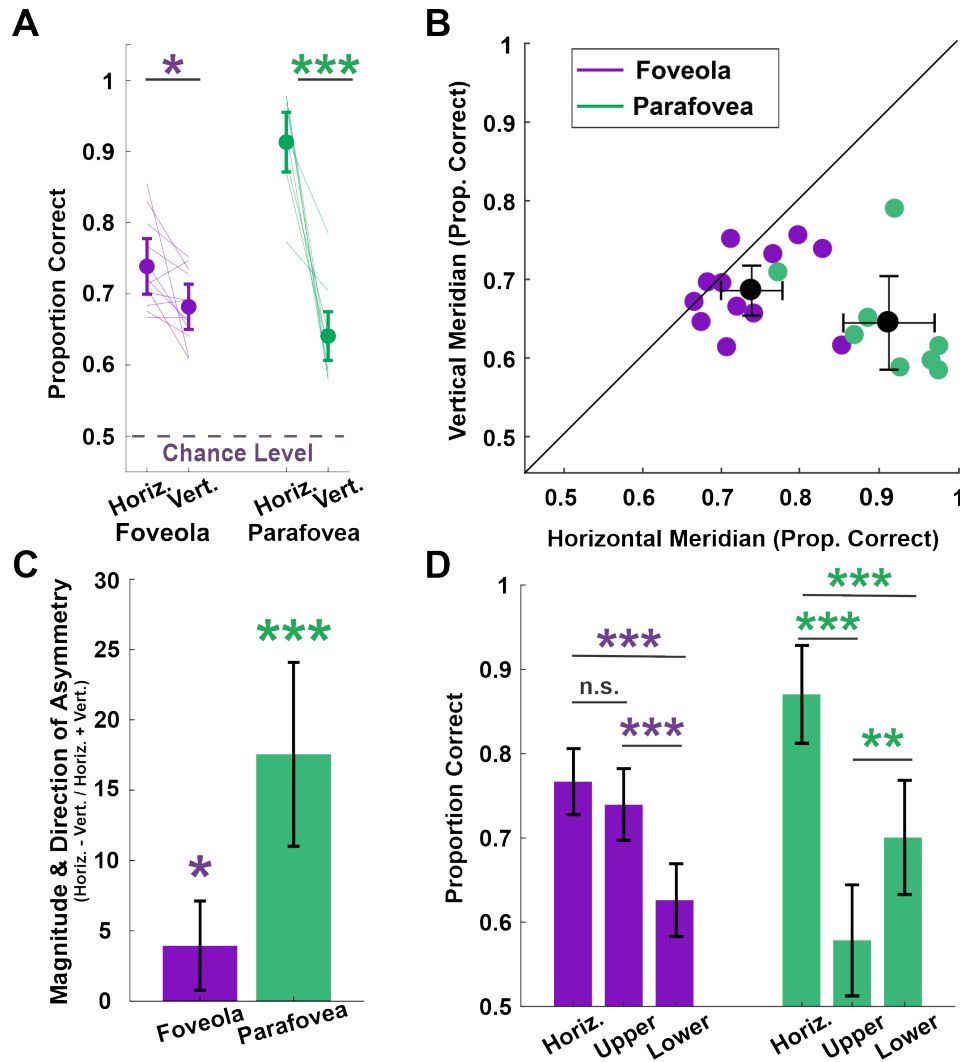


Figure 2: **Horizontal-Vertical Meridian Asymmetry.** **A** and **B**- Average performance along the horizontal (pooled left and right locations) and vertical meridian (pooled top and bottom locations) across subjects for the foveola and the parafovea. Lines in **A** and colored dots in **B** represent individual observers. In **A**, asterisks denote a statistically significant difference (* $P < 0.05$, ** $P \leq 0.01$, *** $P \leq 0.001$, paired t-test $p = 0.02$ foveola, $p = 0.0004$ parafovea). **C**- Magnitude and direction of the horizontal-vertical meridian asymmetry. Asterisks indicate a statistically significant difference from zero (one sample t-test $p = 0.02$ foveola, $p = 0.0004$ parafovea). **D**- Average performance along the horizontal meridian compared to the upper and lower vertical meridian performance for the foveola and the parafovea. Asterisks denote statistically significant differences (one-way ANOVA, $p = 0.0001$ foveola, $p < 0.0001$ parafovea). All Error bars are 95% confidence intervals.

lower vertical: $70\% \pm 7\%$; upper vertical: $58\% \pm 7\%$). However, in the foveola condition, the horizontal-vertical meridian asymmetry was mainly the result of a drop in performance in the lower vertical meridian ($F(2,11) = 13.29$, $p = 0.0002$; $BF = 106.35$; horizontal: $74\% \pm 4\%$; lower vertical: $63\% \pm 4\%$; upper vertical: $74\% \pm 7\%$; Figure 2D).

There was no statistically significant difference in reaction times for stimuli presented along the vertical vs horizontal meridian in the foveola ($Z = -1.2990$, $p = 0.1939$, Wilcoxon rank-sum test), and in the parafovea reaction times were faster for stimuli presented along the horizontal meridian (horizontal: $367\text{ms} \pm 125\text{ms}$; vertical: $524\text{ms} \pm 180\text{ms}$; $Z = -2.15$, $p = 0.031$, Wilcoxon rank-sum test), indicating that the reported asymmetries in visual discrimination are not due to a speed accuracy trade-off.

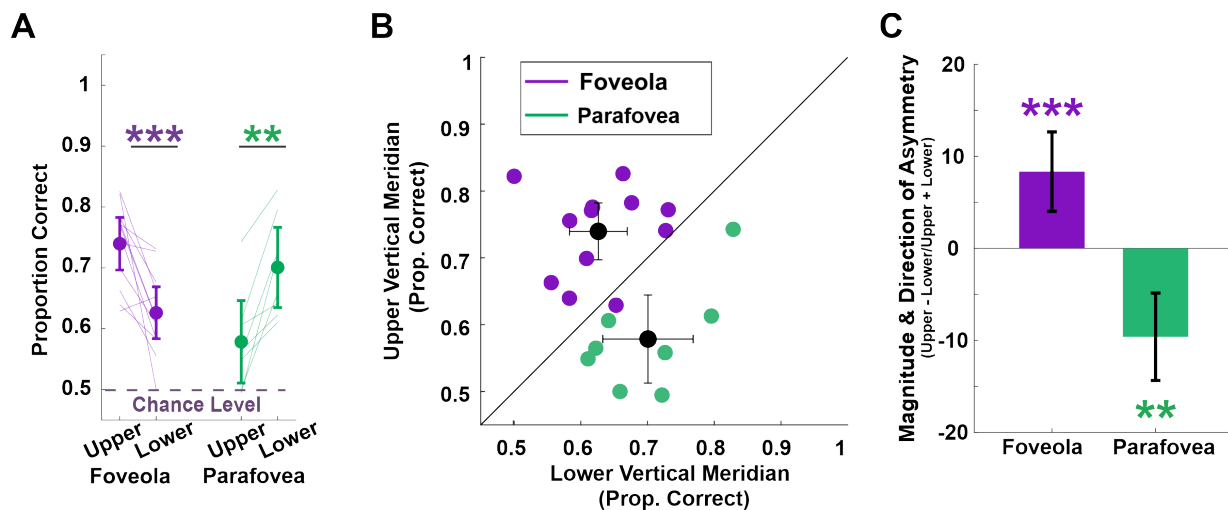


Figure 3: **Vertical Meridian Asymmetry.** Conventions are the same as in Fig. 2. **A and B-** Average performance along the upper and lower vertical meridian across subjects. In **A**, asterisks denote a statistically significant difference (paired t-test, $p = 0.001$ foveola, $p = 0.002$ parafovea). **C-** Magnitude and direction of the vertical meridian asymmetry. Asterisks indicate a statistically significant difference from zero (one sample t-test, $p = 0.001$ foveola, $p = 0.002$ parafovea). All error bars are 95% confidence intervals.

Besides the horizontal-vertical asymmetry, differences in visual perception are also reported along the vertical meridian. Previous research has consistently shown that in the parafovea and perifovea sensitivity is higher in the lower than the upper vertical meridian (e.g.,^{23,18,19,26,29,60,61}). Our findings in the parafovea are in line with the literature (Fig. 3A – B; lower: $70\% \pm 7\%$ upper: $58\% \pm 7\%$; two-tailed paired t-test: $t(7) = -4.90$, $p = 0.002$; $BF = 26.21$; Cohen's $d = 1.35$). In the central fovea, we reported an asymmetry of comparable magnitude (fovea: $11\% \pm 9\%$ and parafovea: $12\% \pm 7\%$), indicating that not all asymmetries are attenuated in this region. Remarkably, the pattern of asymmetry reversed in the foveola (Fig. 3C); visual discrimination was better in the upper than the lower vertical meridian (upper: $73\% \pm 4\%$ vs. lower: $63\% \pm 4\%$; two-tailed paired t-test: $t(11) = 4.32$, $p = 0.001$; $BF = 34.07$; Cohen's $d = 1.56$). When comparing reaction times in the lower and upper vertical meridians for the foveola and parafovea, there was no statistically significant difference (foveola: $Z = -1.18$, $p = 0.24$; parafovea: $Z = 0.9977$, $p = 0.32$, Wilcoxon rank-sum test), indicating that the results were not due to a speed-accuracy trade off.

To examine the visual performance fields with finer resolution, visual discrimination was also tested at intercardi-

nal locations. As reported in some studies (e.g.,^{18,23}), the most noticeable feature of the parafovea and perifovea performance field was the enhancement of performance along the horizontal meridian, giving the performance field an oblong shape (Fig. 4A). The performance field in the central fovea, in contrast, is less oblong and it is mainly characterized by an upper vertical meridian enhancement (Fig. 4A). Performance between the upper and lower intercardinal locations were comparable for the foveola upper: 73% ± 4%, lower: 68% ± 9%; two tailed paired t-test: $t(11) = 1.62$, $p = 0.13$; BF = 1.25 for the null hypothesis; Cohen's D = 0.51) and the parafovea (upper: 65% ± 8%, lower: 73% ± 13%; two tailed paired t-test: $t(7) = -2.00$, $p = 0.085$; BF = 0.78 for the null hypothesis; Cohen's D = 0.65). This result is consistent with findings in the parafovea and perifovea^{18,19,23,24,41,29}.

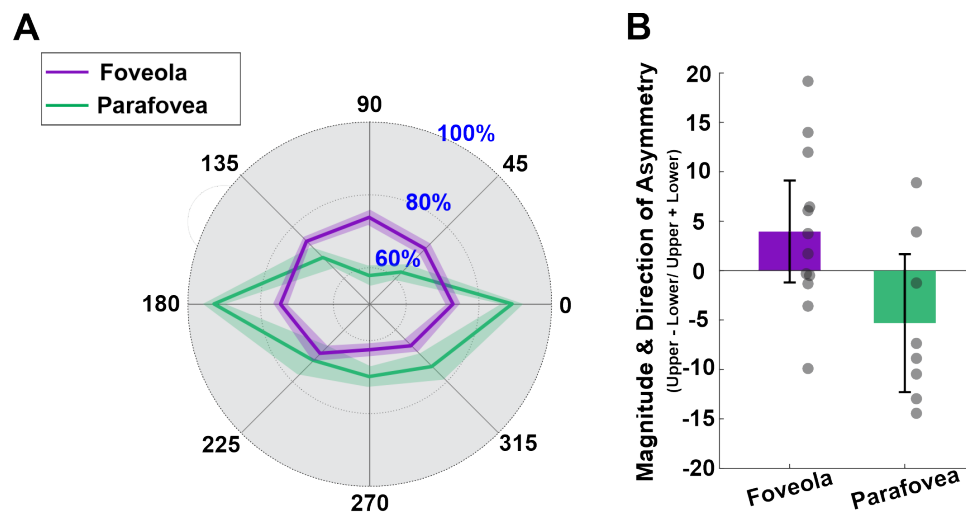


Figure 4: Performance fields in the foveola and parafovea. **A**- The visual performance field in the foveola (purple) and parafovea (green). Each angle represents one tested location. Numbers along the radial direction represent percent correct, and the shaded regions represent SEM. The lines connect the average performance across subjects for the different locations tested. **B**- Magnitude and direction of the asymmetry between the upper intercardinal locations (locations at 45 and 135 deg) and the lower intercardinal locations (locations at 225 and 315 deg). Filled circles represent individual observers. Error bars are 95% confidence intervals.

Discussion

It is typical to characterize extrafoveal vision at different eccentricities rather than as a whole, as many functions gradually decrease as stimulus information is presented more peripherally^{62,63,64} (see^{65,66}, for reviews). However, examining foveolar vision as a whole is common practice. Whereas this may seem justified by the fact that the central fovea covers only a tiny (<0.01%) portion of the visual field, it is at odds with the fact that the foveola is vastly overrepresented in the primary visual cortex, which dedicates 8% of its surface area to the processing of the visual input coming from this region⁴⁵. Moreover, cone density^{11,12,14} and fine visual discrimination^{51,52} have

been shown to decline just a few arcminutes away from the preferred retinal locus of fixation. Therefore, foveolar vision is less homogeneous than usually assumed.

Here, we show that foveolar vision not only changes with eccentricity but also varies around the polar angles of the visual field projecting onto this region, as is the case extrafoveally (see¹⁷ for a review). Specifically, we found that discriminating stimuli located degrees below, compared to above, the center of gaze is easier, whereas discriminating stimuli just a few arcminutes below versus above the center of gaze proves more challenging. This foveal asymmetry, although comparable in magnitude, is opposite in direction to the corresponding asymmetry in the extrafoveal visual field. In general, the overall shape of the parafoveal performance field is oblong along the horizontal meridian, whereas the foveolar performance field is primarily enhanced along the upper vertical meridian.

The horizontal-vertical meridian asymmetry has been reported in parafovea and perfovea studies (e.g.,^{18,19,20,21,22,23,24,25,26,27}). Notably, this parafoveal asymmetry is more prominent in this study than in many previous studies. This difference may be due to differences in stimulus parameters –stimuli used in previous work are larger and often limited to specific spatial frequencies– and the presence of the placeholders, which could have been perceived as distractors –as asymmetries become more pronounced with distractors^{18,41}. Ultimately, these results show that not only is the foveola characterized by visual asymmetries, but also that these asymmetries are unique in the central most 1 deg of the visual field.

As discussed in the Introduction, extrafoveal asymmetries are pervasive and have been shown across various visual tasks and stimulus parameters, raising the question of where along the visual processing pipeline these asymmetries emerge. The first factor that could influence the visual asymmetries are the optics of the eye. Optical aberrations are not symmetric along the visual field meridians⁶⁷, and horizontal/vertical astigmatism and coma vary as a function of polar angle⁶⁸. Specifically, the magnitude of vertical coma gradually decreases from the inferior to superior retina (across -18 to 18 deg), resulting in more optical distortion from vertical coma in the upper compared to the lower vertical meridian⁶⁸. In addition to optical factors, at the anatomical level, the extrafoveal retina is characterized by higher cone^{69,70,71} and retinal ganglion cell¹³ density along the horizontal than the vertical meridian. Whereas retinal cone density contributes towards the horizontal-vertical meridian asymmetry, no difference in cone density has been reported along the vertical meridian. However, the density of mid-retinal ganglion cells (mRGCs) is higher along the superior retina, which projects to the lower visual field, compared to the inferior retina¹³. Moreover, in the mid-periphery, the convergence of cones to mRGCs is minimal along the horizontal meridian but is the greatest along the inferior retina¹³, resulting in greater information loss for stimuli in the upper visual field. This difference aligns with behavioral evidence from this and previous studies.

A computational observer model, however, has shown that optical and retinal factors account for about 40% of the behavioral horizontal-vertical asymmetry and about 10% of the behavioral vertical meridian asymmetry, and that they are amplified at later processing stages in the visual cortex^{72,73}. In the primary visual cortex

asymmetric differences in BOLD response⁷⁴, population receptive field size^{75,17}, and cortical surface area^{76,8,77,17} have been reported. Specifically, for a given eccentricity range, the horizontal meridian can have up to 80% greater cortical surface area than the vertical meridian, and a similar pattern is seen for the lower vs. upper vertical meridian^{15,8,77,17}. Although further investigation is necessary to elucidate the degree to which the visual cortex influences perceptual asymmetries, factors from the retina to the cortex increasingly contribute to the reported visual asymmetries.

What factors influence foveal asymmetries? Unlike in the extrafovea, optical aberrations in the foveola are constant^{48,49,50}. Therefore, we can exclude the influence of optics on foveolar asymmetries. However, retinal factors could play a role in shaping these perceptual asymmetries. Midget retinal ganglion cells (mRGC) have a 1:1 mapping with retinal cone cells⁴⁴, and thus neither mRGC density nor cone-to-mRGC convergence should impact the pattern of asymmetries. It has been observed that the foveola exhibits similar asymmetries in cone density to those in the extrafoveal retina, with a higher cone density along the horizontal than the vertical meridian^{12,10}. This is consistent with our findings that fine visual discrimination is better along the horizontal vs. the vertical meridian. However, like in extrafovea, the foveola shows no differences in cone density along the vertical meridian¹². Therefore, it would seem that cone density alone cannot account for the visual asymmetries observed in the foveola.

Importantly, changes in cone density with eccentricity are generally defined with respect to the peak cone density (PCD) location. However, this location does not coincide with the retinal projection of the center of gaze. The center of gaze on the retina is considered as the preferred retinal locus of fixation (PRL), which can be quantitatively defined as the median retinal location of a stimulus during fixation. Notably, there is an offset between the PRL and the point of highest cone density^{78,12,79,80,81,82,83,47}. Specifically, the PRL is shifted nasally and superiorly from the cone density centroid (CDC)—the centroid of the region with highest cone density—by approximately 5 arcminutes¹². Although this is a small shift, it introduces systematic asymmetries in cone density between the superior vs. inferior retina. Therefore, if eccentricity is defined with respect to PRL rather than from the CDC location, cone density is higher along the inferior retina, corresponding to the upper visual field, than along the superior retina. Although the overall performance was comparable at the intercardinal locations due to relatively large individual variability, this difference in cone density below vs. above the preferred retinal locus could potentially contribute to the vertical meridian asymmetry observed in the foveola. It is likely that subsequent stages of processing in the visual cortex further contribute to the foveolar perceptual asymmetries. Yet currently, unlike in extrafoveal vision, nothing is known about possible cortical asymmetries in the processing of foveolar visual input.

Visual sensitivity differences at isoeccentric locations along different directions may serve functional purposes in vision. A horizontal enhancement could be beneficial for socialization with other people at the same height range as faces are commonly located along the horizontal meridian. This asymmetry is also advantageous for reading, both in the fovea and parafovea, as humans can extract words 12-15 letters ahead of the fixated word along

the horizontal meridian^{84,85}. Interestingly, the horizontal-vertical meridian asymmetry is present in both children and adults⁸⁶, suggesting that it may develop early in life or even be present from birth. However, the vertical meridian asymmetry is absent in children, both in behavior⁸⁶ and cortical surface area¹⁷; behaviorally, it emerges in adolescence⁸⁷. A lower vertical visual field enhancement might be beneficial as the objects that we typically interact with are usually located below our center of gaze⁸⁸; however, they are no longer present at intercardinal locations^{18,19,23,24,41,89}.

Whereas there are no clear functional advantages for the vertical meridian asymmetry at the foveal scale, this asymmetry may be related to oculomotor factors. Specifically, it has been shown that upward saccades greater (but not smaller^{60,30,27,61,90}) than 10 degrees tend to undershoot, whereas downward saccades of the same amplitude tend to overshoot the target stimuli⁹¹. As a result, the foveated target falls above the center of gaze every time a large vertical saccade, either upward or downward, is performed. Therefore, better fine visual discrimination in the upper foveal visual field may be advantageous in these circumstances.

What is the effect of attention on the foveal asymmetries? Covert attention enhances visual performance at the attended location (see⁹² for a review). In the extrafovea, exogenous attention enhances sensitivity uniformly across isoeccentric locations, thereby preserving the magnitude and pattern of the visual asymmetries^{18,19,39,40}. Interestingly, despite generally being characterized by a more flexible deployment^{93,89} endogenous attention was also found to increase the performance field uniformly^{41,42}. Therefore, covert spatial attention allocates comparable resources at all attended locations regardless of whether they are along the horizontal or vertical meridian in the extrafovea. It has been established that attention can be selectively deployed within the foveola, both endogenously⁹⁴ and exogenously⁹⁵. Yet, unlike in the extrafovea, it is not known whether fine scale attention has an effect on foveal asymmetries.

In conclusion, using a high-precision eyetracker to investigate visual performance at selected locations across the 1-degree foveola, this study revealed that foveolar vision is characterized by visual asymmetries in fine visual discrimination. Whereas the magnitude of the horizontal-vertical asymmetry was attenuated compared to the corresponding parafoveal asymmetry, the magnitude of the asymmetry along the vertical meridian (i.e., upper vs lower) was comparable in both conditions. Remarkably, however, the direction of the vertical asymmetry was reversed in the fovea indicating that distinct mechanisms are at play at this scale. This difference may be the result of fixation behavior leading to changes in cone sampling above vs below the fixated location, given the slight offset between the peak cone density location on the retina and the preferred retinal locus, or it may arise from a different cortical representation of foveal input at the level of V1 and beyond. Importantly, these results further emphasize the need to consider foveal vision not as a uniform entity, but as one characterized by significant non-uniformities that shape perception of fine detail.

References

1. Harry G Randall, Darlene J Brown, and Louise L Sloan. Peripheral visual acuity. *Archives of Ophthalmology*, 75(4):500–504, 1966.
2. Gerald Westheimer. Scaling of visual acuity measurements. *Archives of Ophthalmology*, 97(2):327–330, 1979.
3. Michel Millodot, Chris A Johnson, Anne Lamont, and Herschel W Leibowitz. Effect of dioptics on peripheral visual acuity. *Vision Research*, 15(12):1357–1362, 1975.
4. JP Rijdsdijk, JN Kroon, and GJ Van der Wildt. Contrast sensitivity as a function of position on the retina. *Vision research*, 20(3):235–241, 1980.
5. MJ Wright and A Johnston. Spatiotemporal contrast sensitivity and visual field locus. *Vision Research*, 23(10):983–989, 1983.
6. Daniel R Coates, Jeremy M Chin, and Susana TL Chung. Factors affecting crowded acuity: Eccentricity and contrast. *Optometry and vision science: official publication of the American Academy of Optometry*, 90(7), 2013.
7. Jonathan C Horton and William F Hoyt. The representation of the visual field in human striate cortex: a revision of the classic holmes map. *Archives of Ophthalmology*, 109(6):816–824, 1991.
8. Marc M Himmelberg, Jan W Kurzawski, Noah C Benson, Denis G Pelli, Marisa Carrasco, and Jonathan Winawer. Cross-dataset reproducibility of human retinotopic maps. *Neuroimage*, 244:118609, 2021.
9. Noah C Benson, Jennifer MD Yoon, Dylan Forenzo, Stephen A Engel, Kendrick N Kay, and Jonathan Winawer. Variability of the surface area of the v1, v2, and v3 maps in a large sample of human observers. *Journal of Neuroscience*, 42(46):8629–8646, 2022.
10. Christine A Curcio, Kenneth R Sloan Jr, Orin Packer, Anita E Hendrickson, and Robert E Kalina. Distribution of cones in human and monkey retina: individual variability and radial asymmetry. *Science*, 236(4801):579–582, 1987.
11. Robert F Cooper, Melissa A Wilk, Sergey Tarima, and Joseph Carroll. Evaluating descriptive metrics of the human cone mosaic. *Investigative Ophthalmology & Visual Science*, 57(7):2992–3001, 2016.
12. Jenny L Reiniger, Niklas Domdei, Frank G Holz, and Wolf M Harmening. Human gaze is systematically offset from the center of cone topography. *Current Biology*, 31(18):4188–4193, 2021.
13. Andrew B Watson. A formula for human retinal ganglion cell receptive field density as a function of visual field location. *Journal of Vision*, 14(7):15–15, 2014.

14. Christine A Curcio, Kenneth R Sloan, Robert E Kalina, and Anita E Hendrickson. Human photoreceptor topography. *Journal of Comparative Neurology*, 292(4):497–523, 1990.
15. Noah C Benson, Keith W Jamison, Michael J Arcaro, An T Vu, Matthew F Glasser, Timothy S Coalson, David C Van Essen, Essa Yacoub, Kamil Ugurbil, Jonathan Winawer, et al. The human connectome project 7 tesla retinotopy dataset: Description and population receptive field analysis. *Journal of Vision*, 18(13): 23–23, 2018.
16. Serge O Dumoulin and Brian A Wandell. Population receptive field estimates in human visual cortex. *Neuroimage*, 39(2):647–660, 2008.
17. Marc M Himmelberg, Jonathan Winawer, and Marisa Carrasco. Polar angle asymmetries in visual perception and neural architecture. *Trends in Neurosciences*, 2023.
18. Marisa Carrasco, Cigdem P Talgar, and E Leslie Cameron. Characterizing visual performance fields: Effects of transient covert attention, spatial frequency, eccentricity, task and set size. *Spatial Vision*, 15(1):61–75, 2001.
19. E Leslie Cameron, Joanna C Tai, and Marisa Carrasco. Covert attention affects the psychometric function of contrast sensitivity. *Vision Research*, 42(8):949–967, 2002.
20. Michael W Levine and J Jason McAnany. The relative capabilities of the upper and lower visual hemifields. *Vision Research*, 45(21):2820–2830, 2005.
21. Stuart Fuller, Ruby Z Rodriguez, and Marisa Carrasco. Apparent contrast differs across the vertical meridian: Visual and attentional factors. *Journal of Vision*, 8(1):16–16, 2008.
22. Jennifer E Corbett and Marisa Carrasco. Visual performance fields: Frames of reference. *PLoS One*, 6(9): e24470, 2011.
23. Jared Abrams, Aaron Nizam, and Marisa Carrasco. Isoeccentric locations are not equivalent: The extent of the vertical meridian asymmetry. *Vision Research*, 52(1):70–78, 2012.
24. Alex S Baldwin, Tim S Meese, and Daniel H Baker. The attenuation surface for contrast sensitivity has the form of a witch’s hat within the central visual field. *Journal of Vision*, 12(11):23–23, 2012.
25. John A Greenwood, Martin Szinte, Bilge Sayim, and Patrick Cavanagh. Variations in crowding, saccadic precision, and spatial localization reveal the shared topology of spatial vision. *Proceedings of the National Academy of Sciences*, 114(17):E3573–E3582, 2017.
26. Marc M Himmelberg, Jonathan Winawer, and Marisa Carrasco. Stimulus-dependent contrast sensitivity asymmetries around the visual field. *Journal of Vision*, 20(9):18–18, 2020.

27. Nina M Hanning, Marc M Himmelberg, and Marisa Carrasco. Presaccadic attention depends on eye movement direction and is related to v1 cortical magnification. *Journal of Neuroscience*, 44(12), 2024.
28. Cigdem P Talgar and Marisa Carrasco. Vertical meridian asymmetry in spatial resolution: Visual and attentional factors. *Psychonomic Bulletin & Review*, 9:714–722, 2002.
29. Antoine Barbot, Shutian Xue, and Marisa Carrasco. Asymmetries in visual acuity around the visual field. *Journal of Vision*, 21(1):2–2, 2021.
30. Yuna Kwak, Nina M Hanning, and Marisa Carrasco. Presaccadic attention sharpens visual acuity. *Scientific Reports*, 13(1):2981, 2023.
31. Zixuan Wang, Yuki Murai, and David Whitney. Idiosyncratic perception: a link between acuity, perceived position and apparent size. *Proceedings of the Royal Society B*, 287(1930):20200825, 2020.
32. Michael Jigo and Marisa Carrasco. Attention alters spatial resolution by modulating second-order processing. *Journal of Vision*, 18(7):2–2, 2018.
33. Manfred Mackeben. Sustained focal attention and peripheral letter recognition. *Spatial Vision*, 12(1):51–72, 1999.
34. James Danckert and Melvyn A Goodale. Superior performance for visually guided pointing in the lower visual field. *Experimental Brain Research*, 137:303–308, 2001.
35. Stuart Fuller and Marisa Carrasco. Perceptual consequences of visual performance fields: The case of the line motion illusion. *Journal of Vision*, 9(4):13–13, 2009.
36. Ramakrishna Chakravarthi, Danaï Papadaki, and Jan Krajník. Visual field asymmetries in numerosity processing. *Attention, Perception, & Psychophysics*, 84(8):2607–2622, 2022.
37. Dietrich S Schwarzkopf. Size perception biases are temporally stable and vary consistently between visual field meridians. *i-Perception*, 10(5):2041669519878722, 2019.
38. Leila Montaser-Kouhsari and Marisa Carrasco. Perceptual asymmetries are preserved in short-term memory tasks. *Attention, Perception, & Psychophysics*, 71(8):1782–1792, 2009.
39. Mariel Roberts, Rachel Cymerman, R Theodore Smith, Lynne Kiorpes, and Marisa Carrasco. Covert spatial attention is functionally intact in amblyopic human adults. *Journal of Vision*, 16(15):30–30, 2016.
40. Mariel Roberts, Brandon K Ashinoff, F Xavier Castellanos, and Marisa Carrasco. When attention is intact in adults with adhd. *Psychonomic Bulletin & Review*, 25:1423–1434, 2018.
41. Simran Purokayastha, Mariel Roberts, and Marisa Carrasco. Voluntary attention improves performance similarly around the visual field. *Attention, Perception, & Psychophysics*, 83(7):2784–2794, 2021.

42. Ekin Tünçok, Marisa Carrasco, and Jonathan Winawer. Spatial attention alters visual cortical representation during target anticipation. *BioRxiv*, pages 2024–03, 2024.
43. Antonio Fernández, Rachel Denison, and Marisa Carrasco. Temporal attention improves perception at foveal and parafoveal locations equally. *Journal of Vision*, 18(10):1026–1026, 2018.
44. Helga Kolb, Eduardo Fernandez, and Ralph Nelson. Webvision: the organization of the retina and visual system. [*Internet*], 1995.
45. P Azzopardi and A Cowey. Preferential representation of the fovea in the primary visual cortex. *Nature*, 361(6414):719–721, 1993.
46. Michael Jigo, Daniel Tavdy, Marc M Himmelberg, and Marisa Carrasco. Cortical magnification eliminates differences in contrast sensitivity across but not around the visual field. *elife*, 12:e84205, 2023.
47. Niklas Domdei, Jenny L Reiniger, Frank G Holz, and Wolf M Harmening. The relationship between visual sensitivity and eccentricity, cone density and outer segment length in the human foveola. *Investigative Ophthalmology & Visual Science*, 62(9):31–31, 2021.
48. Phillip Bedggood, Mary Daaboul, Ross Ashman, George Smith, and Andrew Metha. Characteristics of the human isoplanatic patch and implications for adaptive optics retinal imaging. *Journal of Biomedical Optics*, 13(2):024008–024008, 2008.
49. David A Atchison, Nicola Pritchard, and Katrina L Schmid. Peripheral refraction along the horizontal and vertical visual fields in myopia. *Vision Research*, 46(8-9):1450–1458, 2006.
50. Junzhong Liang, David R Williams, and Donald T Miller. Supernormal vision and high-resolution retinal imaging through adaptive optics. *JOSA A*, 14(11):2884–2892, 1997.
51. Martina Poletti, Chiara Listorti, and Michele Rucci. Microscopic eye movements compensate for nonhomogeneous vision within the fovea. *Current Biology*, 23(17):1691–1695, 2013.
52. Janis Intoy and Michele Rucci. Finely tuned eye movements enhance visual acuity. *Nature Communications*, 11(1):795, 2020.
53. Kenneth Holmqvist and Pieter Blignaut. Small eye movements cannot be reliably measured by video-based p-cr eye-trackers. *Behavior Research Methods*, 52:2098–2121, 2020.
54. Rwei-Jr Wu, Ashley M Clark, Michele A Cox, Janis Intoy, Paul C Jolly, Zhetuo Zhao, and Michele Rucci. High-resolution eye-tracking via digital imaging of purkinje reflections. *Journal of Vision*, 23(5):4–4, 2023.
55. Fabrizio Santini, Gabriel Redner, Ramon Iovin, and Michele Rucci. Eyeris: a general-purpose system for eye-movement-contingent display control. *Behavior Research Methods*, 39(3):350–364, 2007.

56. Martina Poletti and Michele Rucci. A compact field guide to the study of microsaccades: Challenges and functions. *Vision Research*, 118:83–97, 2016.
57. Jyrki Rovamo and Veijo Virsu. An estimation and application of the human cortical magnification factor. *Experimental Brain Research*, 37:495–510, 1979.
58. Claudia Cherici, Xutao Kuang, Martina Poletti, and Michele Rucci. Precision of sustained fixation in trained and untrained observers. *Journal of Vision*, 12(6):31–31, 2012.
59. Michele Rucci and Martina Poletti. Control and functions of fixational eye movements. *Annual Review of Vision Science*, 1:499–518, 2015.
60. Nina M Hanning, Marc M Himmelberg, and Marisa Carrasco. Presaccadic attention enhances contrast sensitivity, but not at the upper vertical meridian. *Isience*, 25(2), 2022.
61. Yuna Kwak, Zhong-Lin Lu, and Marisa Carrasco. How the window of visibility varies around polar angle. *bioRxiv*, 2024.
62. Stuart M Anstis. Chart demonstrating variations in acuity with retinal position. *Vision Research*, 14(7): 589–592, 1974.
63. JS Pointer and RF Hess. The contrast sensitivity gradient across the human visual field: With emphasis on the low spatial frequency range. *Vision Research*, 29(9):1133–1151, 1989.
64. J Gordon Robson and Norma Graham. Probability summation and regional variation in contrast sensitivity across the visual field. *Vision Research*, 21(3):409–418, 1981.
65. Hans Strasburger, Ingo Rentschler, and Martin Jüttner. Peripheral vision and pattern recognition: A review. *Journal of Vision*, 11(5):13–13, 2011.
66. Katharina Anton-Erxleben and Marisa Carrasco. Attentional enhancement of spatial resolution: linking behavioural and neurophysiological evidence. *Nature Reviews Neuroscience*, 14(3):188–200, 2013.
67. W Neil Charman and David A Atchison. Decentred optical axes and aberrations along principal visual field meridians. *Vision Research*, 49(14):1869–1876, 2009.
68. Dibyendu Pusti, Chloe Degre Kendrick, Yifei Wu, Qiuzhi Ji, Hae Won Jung, and Geunyoung Yoon. Widefield wavefront sensor for multidirectional peripheral retinal scanning. *Biomedical Optics Express*, 14(8):4190–4204, 2023.
69. Richard Legras, Alain Gaudric, and Kelly Woog. Distribution of cone density, spacing and arrangement in adult healthy retinas with adaptive optics flood illumination. *PLoS One*, 13(1):e0191141, 2018.

70. Hongxin Song, Toco Yuen Ping Chui, Zhangyi Zhong, Ann E Elsner, and Stephen A Burns. Variation of cone photoreceptor packing density with retinal eccentricity and age. *Investigative Ophthalmology & Visual Science*, 52(10):7376–7384, 2011.
71. EM Wells-Gray, SS Choi, A Bries, and N Doble. Variation in rod and cone density from the fovea to the mid-periphery in healthy human retinas using adaptive optics scanning laser ophthalmoscopy. *Eye*, 30(8): 1135–1143, 2016.
72. Eline R Kupers, Marisa Carrasco, and Jonathan Winawer. Modeling visual performance differences ‘around’ the visual field: A computational observer approach. *PLoS Computational Biology*, 15(5):e1007063, 2019.
73. Eline R Kupers, Noah C Benson, Marisa Carrasco, and Jonathan Winawer. Asymmetries around the visual field: From retina to cortex to behavior. *PLoS Computational Biology*, 18(1):e1009771, 2022.
74. Taosheng Liu, David J Heeger, and Marisa Carrasco. Neural correlates of the visual vertical meridian asymmetry. *Journal of Vision*, 6(11):12–12, 2006.
75. Maria Fatima Silva, Jan W Brascamp, Sónia Ferreira, Miguel Castelo-Branco, Serge O Dumoulin, and Ben M Harvey. Radial asymmetries in population receptive field size and cortical magnification factor in early visual cortex. *NeuroImage*, 167:41–52, 2018.
76. Noah C Benson, Eline R Kupers, Antoine Barbot, Marisa Carrasco, and Jonathan Winawer. Cortical magnification in human visual cortex parallels task performance around the visual field. *Elife*, 10:e67685, 2021.
77. Marc M Himmelberg, Jonathan Winawer, and Marisa Carrasco. Linking individual differences in human primary visual cortex to contrast sensitivity around the visual field. *Nature Communications*, 13(1):3309, 2022.
78. Nicole M Putnam, Heidi J Hofer, Nathan Doble, Li Chen, Joseph Carroll, and David R Williams. The locus of fixation and the foveal cone mosaic. *Journal of Vision*, 5(7):3–3, 2005.
79. Norick R Bowers, Josselin Gautier, Samantha Lin, and Austin Roorda. Fixational eye movements in passive versus active sustained fixation tasks. *Journal of Vision*, 21(11):16–16, 2021.
80. Kaccie Y Li, Pavan Tiruveedhula, and Austin Roorda. Intersubject variability of foveal cone photoreceptor density in relation to eye length. *Investigative Ophthalmology & Visual Science*, 51(12):6858–6867, 2010.
81. Melissa A Wilk, Adam M Dubis, Robert F Cooper, Phyllis Summerfelt, Alfredo Dubra, and Joseph Carroll. Assessing the spatial relationship between fixation and foveal specializations. *Vision Research*, 132:53–61, 2017.
82. Yiyi Wang, Nicolas Bensaid, Pavan Tiruveedhula, Jianqiang Ma, Sowmya Ravikumar, and Austin Roorda. Human foveal cone photoreceptor topography and its dependence on eye length. *Elife*, 8:e47148, 2019.

83. Markku Kilpeläinen, Nicole M Putnam, Kavitha Ratnam, and Austin Roorda. The retinal and perceived locus of fixation in the human visual system. *Journal of Vision*, 21(11):9–9, 2021.
84. Keith Rayner, Timothy J Slattery, and Nathalie N Bélanger. Eye movements, the perceptual span, and reading speed. *Psychonomic Bulletin & Review*, 17(6):834–839, 2010.
85. Julia Justino and Régine Kolinsky. Eye movements during reading in beginning and skilled readers: Impact of reading level or physiological maturation? *Acta Psychologica*, 236:103927, 2023.
86. Marisa Carrasco, Mariel Roberts, Caroline Myers, and Lavanya Shukla. Visual field asymmetries vary between children and adults. *Current Biology*, 32(11):R509–R510, 2022.
87. Marisa Carrasco, Caroline Myers, and Mariel Roberts. Visual field asymmetries vary between adolescents and adults. *BioRxiv*, pages 2023–03, 2023.
88. Fred H Previc. Functional specialization in the lower and upper visual fields in humans: Its ecological origins and neurophysiological implications. *Behavioral and Brain Sciences*, 13(3):519–542, 1990.
89. Antoine Barbot and Marisa Carrasco. Attention modifies spatial resolution according to task demands. *Psychological Science*, 28(3):285–296, 2017.
90. Xiaoyi Liu, David Melcher, Marisa Carrasco, and Nina M Hanning. Presaccadic preview shapes postsaccadic processing more where perception is poor. *Proceedings of the National Academy of Sciences*, 121(37):e2411293121, 2024.
91. Han Collewyn, Casper J Erkelens, and Robert M Steinman. Binocular co-ordination of human vertical saccadic eye movements. *The Journal of Physiology*, 404(1):183–197, 1988.
92. Marisa Carrasco. Visual attention: The past 25 years. *Vision Research*, 51(13):1484–1525, 2011.
93. Antoine Barbot, Michael S Landy, and Marisa Carrasco. Differential effects of exogenous and endogenous attention on second-order texture contrast sensitivity. *Journal of Vision*, 12(8):6–6, 2012.
94. Martina Poletti, Michele Rucci, and Marisa Carrasco. Selective attention within the foveola. *Nature Neuroscience*, 20(10):1413–1417, 2017.
95. Yue Zhang, Natalya Shelchkova, Rania Ezzo, and Martina Poletti. Transient perceptual enhancements resulting from selective shifts of exogenous attention in the central fovea. *Current Biology*, 31(12):2698–2703, 2021.
96. A Cowey and ET Rolls. Human cortical magnification factor and its relation to visual acuity. *Experimental Brain Research*, 21:447–454, 1974.

97. Marisa Carrasco and Karen S Frieder. Cortical magnification neutralizes the eccentricity effect in visual search. *Vision Research*, 37(1):63–82, 1997.
98. Hans Strasburger, Ingo Rentschler, and Lewis O Harvey Jr. Cortical magnification theory fails to predict visual recognition. *European Journal of Neuroscience*, 6(10):1583–1588, 1994.

Methods

Subjects: The experiment included 13 participants (11 naive), including one of the authors, aged 18 or older (mean 24 ± 4.54 years; 8 female) with normal or corrected to normal vision. One subject was removed from the analysis due to performance being at chance level in all conditions tested. Eight of the twelve subjects participated in both conditions (foveola, $n=12$ and parafovea $n=8$). The University of Rochester Institutional Review Boards approved the experiment. All study participants provided consent prior to the study.

Apparatus: Stimuli were displayed on an LCD monitor with a refresh rate of 200 Hz and a spatial resolution of 1920×1080 pixels (Acer Predator XB272). The task was performed monocularly with the right eye while the left eye was patched. To prevent head movements, a unique dental-imprint bite bar and a headrest were used. The right eye's movements were recorded at 340Hz using a Basler-acA2000-340KM-NIR camera. EyeRIS, a custom-developed system that allows flexible gaze contingent display control, was used to render the stimuli⁵⁵. This system acquires eye movement signals from a high precision digital Dual Purkinje Image eyetracker⁵⁴, processes them in real time, and updates the stimulus on the display based on the desired combination of estimated oculomotor variables.

System Calibration: Before the start of each block, subjects align their unique dental-imprint bite bar to the center of monitor, by looking through a set of two pinholes. Once aligned, the subject undergoes two step system calibrations. First, subjects undergo a standard automatic calibration procedure using a 3×3 grid of points. Points were 1.32 degrees apart from each other in the horizontal and vertical directions. The mapping obtained through the automatic calibration was then refined using a custom-made manual calibration procedure^{56,51}. This dual-step calibration allows a more accurate localization of gaze position than standard single-step procedures, improving 2D localization of the line of sight by approximately a factor of three on each axis^{51,56}. During the experiment, the manual calibration procedure was then repeated for the central fixation marker before each trial to compensate for possible small head movements introducing errors in gaze localization.

Experimental Protocol: After calibration, subjects started the trial by pressing a button. The stimulus array consisted of four 7×7 arcminute squares at 0.33 deg (foveola condition) or 22×22 arcminute squares at 4.5 deg (parafovea condition) away from the central fixation square (5×5 arcmin). These placeholders could be either located along the cardinal directions or along four intercardinal directions. Cardinal and intercardinal directions were tested in separate blocks for a total of eight tested locations. While subjects maintained fixation on a central marker, a small bar (2×7 arcmin or 6×20 arcmin) tilted ± 45 deg was briefly presented for 50 ms at one of four possible locations. The parafoveal stimuli were magnified according to the cortical magnification factor at that eccentricity⁵⁷, similarly to the way is calculated in prior studies^{96,97,46,98}. Subjects performed a 2AFC orientation discrimination task. Stimuli contrast was adjusted using the method of constant stimuli during a preliminary session to yield an overall performance of 70% correct responses across the eight locations tested. Stimuli contrast was then maintained at this level throughout the following experimental sessions. After 250 ms

from target offset, a green response cue (2×7 arcmin or 6×20 bar) appeared for 100ms. Subjects had four seconds to report the orientation of the target stimulus using a joystick.

Analysis of oculomotor data: Only trials with optimal, uninterrupted tracking and free from saccades and microsaccades during the period of interest (50ms before target onset to 50ms after target offset) were selected for data analysis. When retinal stabilization was used trials characterized with drift amplitudes larger than 100 arcmin were removed to eliminate instances in which subjects attempted to chase the stabilized stimulus (0.2% of trials for subject 1 and 1.2% for subject 5). When stimuli were viewed without retinal stabilization in the foveola condition, trials in which the gaze was ≥ 10 arcmin away from the central fixation marker during the period of interest (50ms before target onset to 50ms after target offset) were discarded to ensure that stimuli were presented at the desired eccentricity (see Methods) (on average $10\% \pm 7\%$ of trials were removed for this reason). This criterion was more relaxed in the Parafoveal condition, as the stimuli were farther away from the center of gaze. Trials in which gaze was ≥ 30 arcmin away from the central fixation marker during the period of interest were discarded (on average $2\% \pm 1\%$ of trials).

Analysis of behavioral data and statistics: Besides characterizing performance as percent of correct responses we also calculated performance as d-prime. Hit and false alarm rates were corrected for response bias (Stanislaw and Todorov, 1999). Overall, we found the results based on the d-prime performance in agreement with those based on percent correct reported in the main text. Both conditions, showed a significant horizontal-vertical meridian asymmetry; participants were on average $58\% \pm 24\%$ better at discriminating stimuli along the horizontal than the vertical meridian in the parafovea (horizontal = $3 d' \pm 1 d'$; vertical = $0.75 d' \pm 0.4 d'$; two-tailed paired t-test: $t(7) = 5.43$, $p = 0.0001$; BF = 41.96; Cohen's $d = 2.86$), and $15\% \pm 18\%$ and better in the foveola (horizontal: $1.34 d' \pm 0.41 d'$; vertical: $0.97 d' \pm 0.28 d'$; two-tailed paired t-test: $t(11) = 2.69$, $p = 0.021$; BF = 3.28; Cohen's $d = 0.98$). Additionally, our findings show that the sensitivity in the lower vertical meridian was higher than in the upper vertical meridian (lower: $1.12 d' \pm 0.5 d'$ upper: $0.42 d' \pm 0.42 d'$; two-tailed paired t-test: $t(7) = -4.94$, $p = 0.002$; BF = 27.05; Cohen's $d = 1.35$). Again, this pattern was reversed in the foveolar condition; the upper vertical meridian was more sensitive than the lower vertical meridian (upper: $1.36 d' \pm 0.42$ vs. lower: $0.67 d' \pm 0.38 d'$; two-tailed paired t-test: $t(11) = 4.46$, $p = 0.001$; BF = 41.15; Cohen's $d = 1.58$.)

All analyses were performed in MATLAB. ANOVAs, post-hoc multiple comparison tests, paired t-tests and Cohen's D calculations were performed using MATLAB's statistical toolbox. To quantify the magnitude of the effects we calculated the BayesFactor for ANOVA's and t-tests using the Bayesfactor MATLAB toolbox (<https://zenodo.org/badge/latestdoi/162604707>)

Acknowledgements: This work was funded by NIH R01 EY029788-01 to MP, NIH training grant T32EY007125 to SJ, EY001319 and NIH NEI Grant R01-EY-027401 to MC.